

# Side-chain crystallization and mobility of poly( $\gamma$ -stearyl-L-glutamate)

F. J. Romero Colomer\* and J. L. Gómez Ribelles†‡

\*Department of Applied Physics and †Laboratory of Thermodynamics and Physical Chemistry, ETSII, University Polytechnic of Valencia, Camino de Vera S/N, 46020 Valencia, Spain

and J. Lloveras Maciá and S. Muñoz Guerra

Department of Chemical Engineering, ETSIIB, University Polytechnic of Cataluña, Diagonal 647, 08028 Barcelona, Spain  
(Received 2 April 1990; accepted 30 May 1990)

Two phase transitions have been found in poly( $\gamma$ -stearyl-L-glutamate) by using differential scanning calorimetry (d.s.c.) and X-ray diffraction techniques. These transitions define the existence of three phases, A, B and C, in order of increasing temperature. The A–B transition involves both the melting of the side-chain crystallites and the rearrangement of the helices. The kinetics of side-chain crystallization and those of the formation of phase B are determined by d.s.c. The side-chain mobility in phase A has been studied by measuring the dielectric relaxation spectrum of the sample as a function of the degree of crystallization.

(Keywords: poly( $\gamma$ -stearyl-L-glutamate); side-chain crystallization; phase transitions; dielectric relaxation)

## INTRODUCTION

Watanabe *et al.*<sup>1</sup> have made a systematic study of the structure and thermal behaviour of a series of poly(*n*-alkyl-glutamate)s including paraffin side chains of up to 18 carbon atoms. Although the polypeptide backbone adopts the rigid conformation of the  $\alpha$  helix in all cases, it is the constitution of the side chain which actually determines the supramolecular organization of the polymer. A crystalline microphase made up of side chains appears when they contain 10 or more methylene units. Consequently, a biphasic microstructure is generated in which the  $\alpha$  helices become aligned in layers with the side-chain crystallites located between them (phase A). The melting of the paraffin crystallites causes a complete reordering of the microstructure, which usually gives rise to a cholesteric liquid phase (phase C). Although in certain cases evidence exists that the process occurs through an intermediate hexagonal phase made up of double helices (phase B)<sup>1,2</sup>, neither the formation mechanism nor the structure of these phases is in general well characterized. In particular, for poly( $\gamma$ -stearyl-L-glutamate) (PSLG), the microstructure described for phase A is characterized by an interlayer distance of 32.7 Å\*, with approximately half of the polymethylene side chain incorporated in the paraffin microphase with a triclinic structure. Only the transition A–C has been observed in the thermal treatment of this system<sup>1</sup>. Further evidence of the main chain conformation and the side chain crystallization and melting temperature were obtained recently by Yamanobe *et al.*<sup>3</sup> by means

of <sup>13</sup>C nuclear magnetic resonance (n.m.r.) experiments on PSLG.

This paper reports a study on the crystallization process and mobility of the side chains of PSLG using differential scanning calorimetry (d.s.c.), X-ray diffraction and dielectric measurements. It shows that, in keeping with the behaviour observed in other poly( $\gamma$ -alkyl-L-glutamate)s with shorter side chains, an intermediate B phase seems to be adopted by this polymer.

## EXPERIMENTAL

The sample used in this study was supplied by Professor K. Yoshioka of the University of Tokyo. It was obtained by transesterification of poly( $\gamma$ -methyl-L-glutamate) ( $M_v \approx 5 \times 10^4$ ) with stearyl alcohol using hydrogen chloride as the catalyst. The 200 MHz <sup>1</sup>H n.m.r. spectrum is as expected for this polymer and no signal corresponding to the methyl carboxylate group was detected. On the other hand, gel permeation chromatography (g.p.c.) of this sample in dichloromethane proved that the transesterification reaction proceeded with no significant degradation. Elementary analysis proved that a replacement of at least 95% of the methyl ester groups had been achieved.

Films  $\approx 30 \mu\text{m}$  thick were used throughout this work. They were obtained by slow evaporation of a solution of the polymer in dichloromethane. The remaining solvent was removed by immersion in ethanol and drying under vacuum until constant weight was achieved.

The calorimetric measurements were made with a Perkin–Elmer DSC 4 differential scanning calorimeter on a single encapsulated sample. All the thermal treatments were carried out inside the calorimeter. The

\* 1 Å =  $10^{-1}$  nm

‡ To whom correspondence should be addressed

dielectric measurements were made with a capacitor bridge General Radio 1620 Å, using a sample metallized with colloidal silver.

The X-ray diagrams were registered on flat films in a Statton type camera (W. Warhus, Wilmington, DE, USA) using  $K\alpha$  copper radiation filtered with nickel and provided with a temperature control stage. The accuracy of the thermal measurement is  $\pm 5^\circ\text{C}$ . Polymer films were placed with the surface either parallel (edge view) or normal (transverse view) to the X-ray beam direction. Continuous X-ray diffractograms were recorded in a Siemens D-500 diffractometer with  $K\alpha(w)$  radiation provided with a TPK-A Park heating stage and a scintillation counter.

## RESULTS AND DISCUSSION

### Phase transitions in PSLG

The structural changes which occur in PSLG when it is heated from room temperature up to  $120^\circ\text{C}$  have been followed by X-ray diffraction and d.s.c. Figure 1 shows a d.s.c. thermogram in which two transitions at  $\approx 63$  and  $\approx 89^\circ\text{C}$  can be seen. These define the existence of the three phases A, B and C in accordance with the general behaviour observed in poly( $\gamma$ -n-alkyl-L-glutamate)s. The increase in enthalpy associated with the A–B transition is  $\approx 70 \text{ J g}^{-1}$ ; that corresponding to the B–C transition is only  $\approx 1 \text{ J g}^{-1}$ . In both cases the increase in enthalpy was found to depend on the thermal history of the sample, as will be seen later.

An X-ray diagram at  $25^\circ\text{C}$  of a PSLG film registered with the radiation parallel to its surface is shown in Figure 2a. A Debye–Scherrer diagram with the same spacings is obtained when the radiation is incident perpendicular to the surface of the film (Figure 2b). Analysis of these diagrams agrees essentially with the layered structure proposed by Watanabe<sup>1</sup> if it is assumed that the crystallites adopt an uniplanar orientation in the sample. The intense equatorial reflection with a spacing of  $\approx 32 \text{ \AA}$  clearly corresponds to the interlayer distance and characterizes the phase A present at this temperature. Heating above  $63^\circ\text{C}$  causes both the disappearance of every reflection arising from the crystalline paraffin

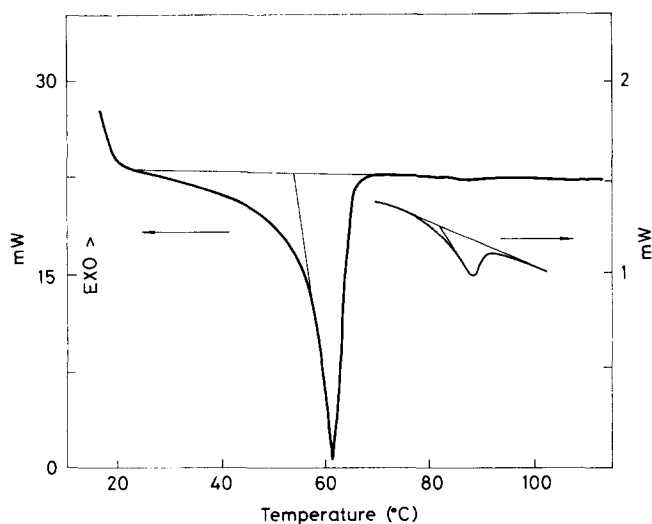


Figure 1 D.s.c. thermogram of a sample of PSLG maintained at  $120^\circ\text{C}$  for 10 min and cooled at  $40^\circ\text{C min}^{-1}$  to  $15^\circ\text{C}$

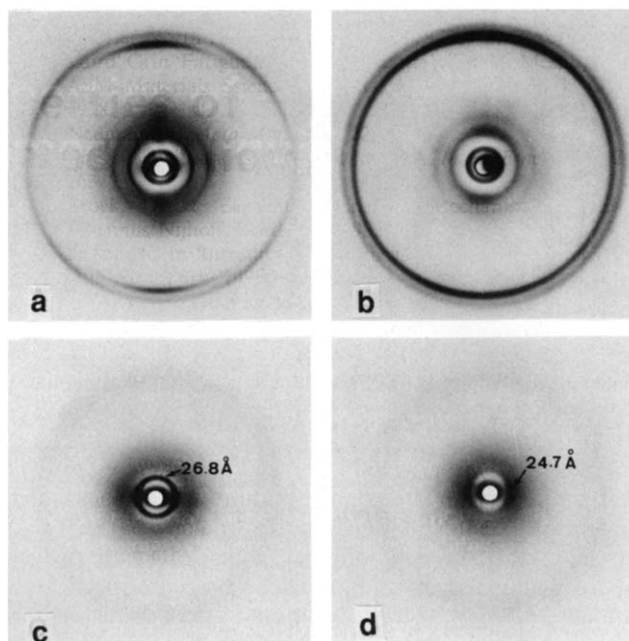
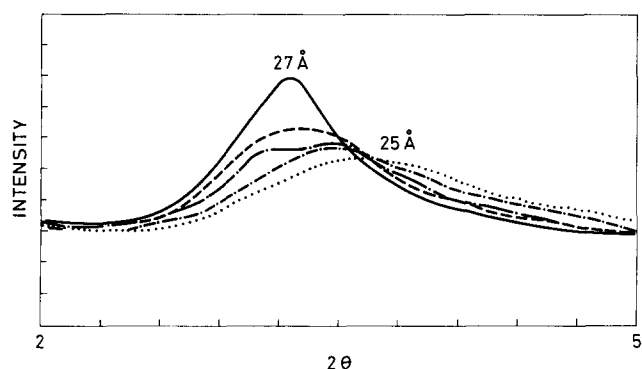


Figure 2 X-ray diagrams obtained from a film of PSLG under the following conditions: (a)  $25^\circ\text{C}$ , edge view; (b)  $25^\circ\text{C}$ , transverse view; (c)  $75^\circ\text{C}$ ; (d)  $120^\circ\text{C}$ . In both (a) and (b) the orientation of the film is vertical

microphase and the shortening of the equatorial spacing to  $26.8 \text{ \AA}$ . A partial loss of orientation is observed in addition (Figure 2c). When the heating process is followed under a polarizing optical microscope, a momentary disappearance of the birefringence is observed at  $63^\circ\text{C}$ . This is spontaneously recovered as soon as the temperature rises by a few degrees. Such an observation suggests that the A–B transition implies not only the melting of the polymethylene side chains but also a rearrangement of the helices within the crystals.

The diagram registered at  $120^\circ\text{C}$  (Figure 2d) consists of a single diffuse reflection centred at  $24.7 \text{ \AA}$ , which seems to indicate that a subsequent microstructural modification must be involved in the B–C transition. Definitive evidence of the displacement of the  $27 \text{ \AA}$  reflection to a spacing of  $24.7 \text{ \AA}$  is obtained by following the evolution of the radial profile of the X-rays diffracted by a film of the sample subjected to temperatures from  $90$  to  $120^\circ\text{C}$  (Figure 3). In the parent polymer, poly( $\gamma$ -dodecyl-L-glutamate), meridional reflections characteristic of a double helix have been observed within the temperature range of the existence of phase B<sup>2</sup>. In PSLG we have not observed changes in the birefringence at temperatures where the B–C transition occurs, which would be expected if a double to single helix conversion had taken place. Moreover the X-ray diagrams obtained in phase B do not show any evidence for a double helix. Although our experimental results are insufficient to characterize the structural forms present in phases B and C, they do allow us to conclude that at temperatures higher than the melting temperature of the side chains, helices are able to arrange themselves in modes defined by spacings at  $26.8$  and  $24.7 \text{ \AA}$ , respectively. Therefore, the thermal transition observed by d.s.c. at  $89^\circ\text{C}$  is made to correspond to the interconversion of these two different arrangements. Such structural change could merely imply a reordering in the packing of the helices due to the different interlocking model followed by the side chains in each case.



**Figure 3** Radial profiles of X-ray diffractograms of PSLG film taken at different temperatures: —, 90; ---, 95; - · - ·, 100; · · · ·, 110; · · · ·, 120°C

X-ray diagrams at room temperature of samples which had been heated previously to 75 or 120°C reveal that phase A is recovered in both cases. It has also been proven by d.s.c. that the thermograms can be reproduced for a similar thermal history beginning with annealing at 120°C. On the contrary, thermal treatments at lower temperatures significantly affect the phase transitions, as described below.

#### Kinetics of the formation of phase B

The evolution of the B–C transition peak with temperature in the range between the two transitions has been followed after different treatment times at 75°C by using d.s.c. The sample was previously heated to 120°C and maintained at that temperature for at least 10 min to eliminate any effect of previous thermal histories. Then it was cooled at 40°C min<sup>-1</sup> to 75°C and maintained at this temperature for a time *t* and finally cooled, at 40°C min<sup>-1</sup> again, to 55°C. Scans were then carried out between 55 and 120°C. *Figure 4a* shows how the peak B–C moves towards higher temperatures with a simultaneous increase of the transition enthalpy (*Figure 4b*) as the treatment time is lengthened. This clearly indicates that the number of helices in phase B increases with treatment time. It can reasonably also be concluded that, in the range of temperatures between the two transitions, the two modes of packing for the helices which we have identified as phase B and phase C must coexist. The considerable spread along the equator displayed by the ≈27 Å reflection in X-ray diagrams taken from samples at temperatures within such a range is in agreement with that interpretation.

#### Kinetics of the crystallization of the side chains

The kinetics of the crystallization of the side chains was studied by carrying out isothermal crystallizations at slightly different temperatures, and also by measuring the melting enthalpy after different thermal histories, including annealing at different temperatures and times.

In the first type of test the sample was heated to 120°C and maintained at this temperature for 10 min. Then it was cooled at 80°C min<sup>-1</sup> to the corresponding crystallization temperature and the flow of heat,  $\dot{Q}$ , was measured as a function of time (*Figure 5*). The value of the heat flow extrapolated to infinite time was taken as the baseline for the integration of these curves<sup>4,5</sup> to obtain the conversion percentage for each crystallization time:

$$X(t) = \int_0^t \dot{Q} dt / \int_0^\infty \dot{Q} dt$$

The values of  $X(t)$  can be adjusted by using the Avrami model<sup>6</sup>

$$1 - X(t) = \exp(-Kt^n)$$

giving a value of 2.5 for the coefficient *n*.

Treatment at temperatures lower than 47.5°C affects both crystallinity and crystalline micromorphology, as shown by the changes observed in the area and shape of the melting peak. The sample was maintained at 120°C for 10 min and then cooled at 40°C min<sup>-1</sup> to 20°C. A thermal scan up to 120°C was taken. *Figure 6a* shows the thermograms obtained after annealing at 30°C. It can be seen that the melting peak for the side chains is not significantly affected either in position or height but a shoulder appears between 30 and 55°C which is representative of the melting of crystals of a significantly smaller size than those formed during cooling (which melt at ≈63°C). Annealing therefore favours the formation of small crystals without enlarging those crystals formed at higher temperatures. On the other hand, treatment at 47.3°C produces an increase in the temperature of the maximum as well as in its intensity, which is interpreted as an increasing in size of the crystals formed

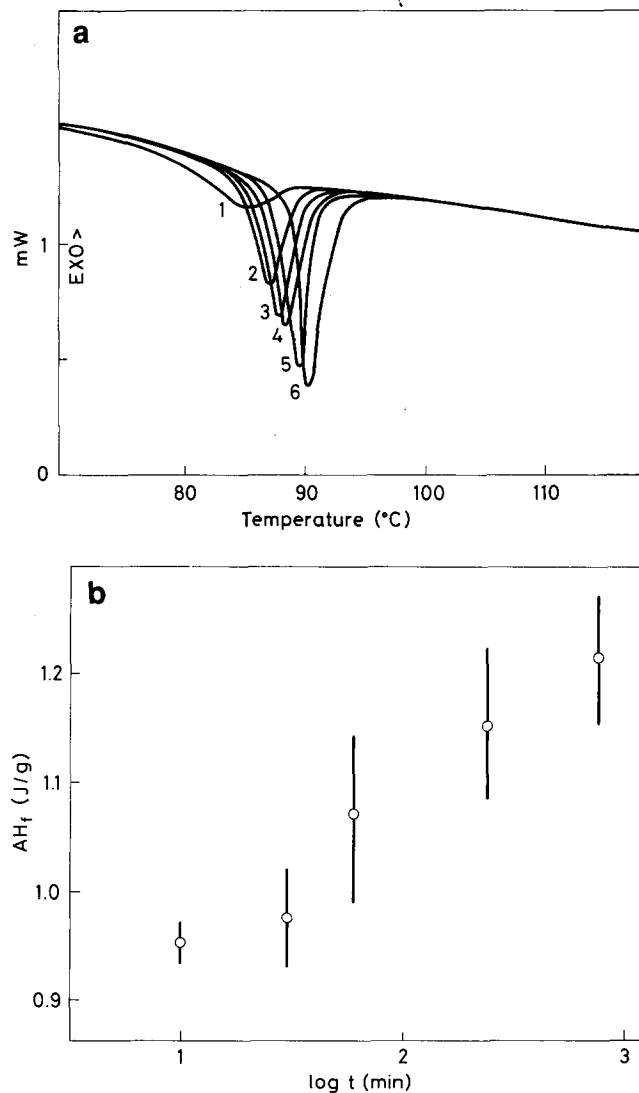


**Figure 4** (a) D.s.c. thermograms near the B–C transition measured after different treatment times at 75°C; 1, 0; 2, 12; 3, 30; 4, 60; 5, 300; 6, 780 min; sweep started at 55°C. (b) Increase of B–C transition enthalpy as a function of treatment time; sweep started at 30°C

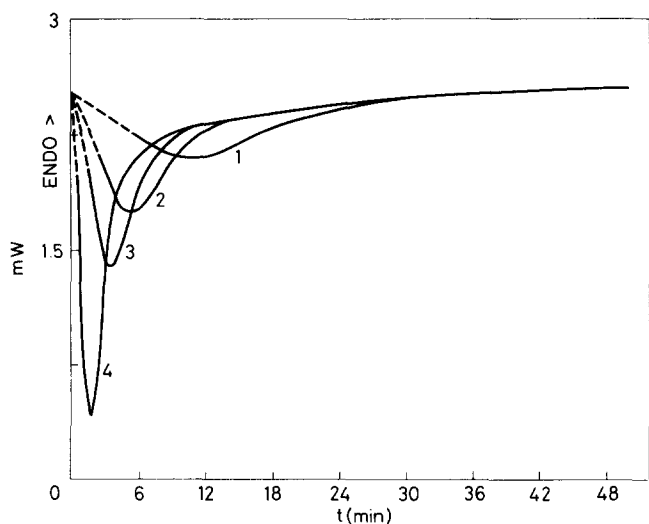


Figure 5 Thermograms of isothermal crystallization of PSLG at different temperatures: 1, 49; 2, 48.5; 3, 48; 4, 47.5°C

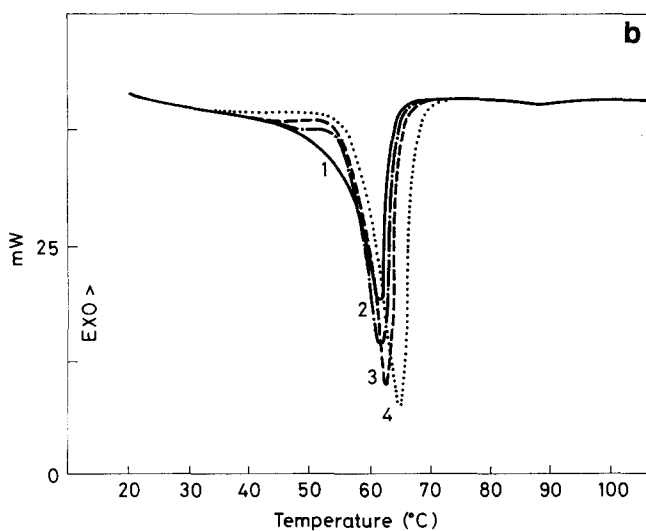
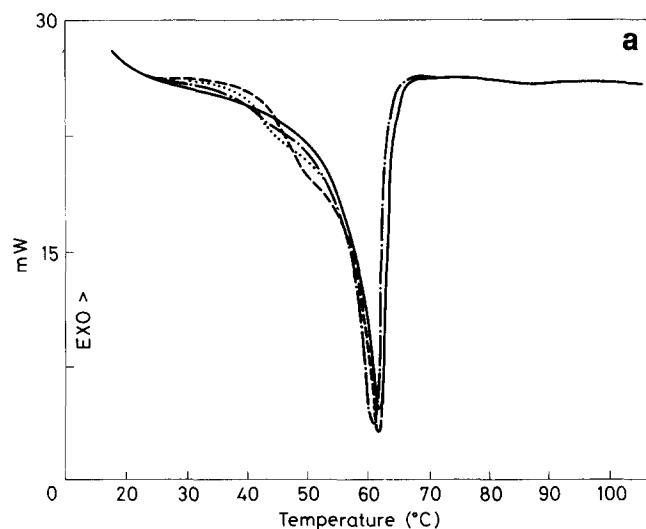


Figure 6 D.s.c. thermograms of PSLG for different treatment times: (a) 30°C; 1, no annealing; 2, 10 min; 3, 60 min; 4, 15 h. (b) 47.3°C; 1, no annealing; 2, 30 min; 3, 15 h; 4, 9 days

during the cooling stage (Figure 6b). In all cases annealing increases the total transition enthalpy due to an increase in the content of crystalline fraction in the sample. Figure 7 shows a practically linear dependency of melting enthalpy on annealing time at temperatures <47.5°C.

The behaviour described coincides qualitatively with

that found in low density polyethylene<sup>7,8</sup>. Obviously the melting temperature in PSLG is considerably lower due to the fact that the crystallites are much smaller. However, the fact that crystallization takes place in a space bounded by the helices and the links in the side chains with the helices limit mobility of the chains does not appear to change qualitatively the kinetics of the crystallization process.

The fraction of the side chains involved in the crystalline phase can be calculated as a quotient of the experimental melting enthalpy and the estimated theoretical fusion enthalpy after the Flory and Vrij<sup>9</sup> formula given for other comb polymers<sup>1,10,11</sup>. Assuming that the total increase in enthalpy measured corresponds to the fusion of the side chains (the small contribution from the rearrangement of the helices accompanying this process may be ignored<sup>12,13</sup>), 32% of the total number of methylene units of the side chains is estimated to participate in the crystalline phase of the sample cooled at 40°C min<sup>-1</sup> from 120°C ( $w_c = 0.32$ ). With annealing, values for  $w_c$  of up to 0.36 have been obtained. This implies that an average of 5.7–6.5 methylene units per side chain are incorporated in the crystalline phase. Dielectric measurements provide further information in relation to this point as they show how the mobility of the chains depends on whether they are in the amorphous or in the crystalline phase.

#### Dielectric relaxations

The dielectric relaxation spectra of poly( $\gamma$ -n-alkyl-L-glutamate)s are characterized by two relaxation processes, known as  $\gamma$  and  $\beta$  in order of increasing

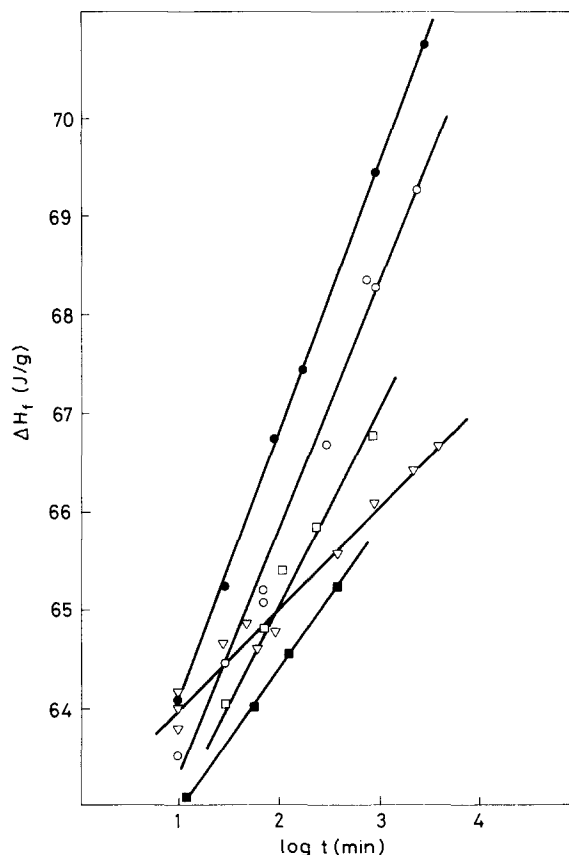


Figure 7 Increase in enthalpy of the A-B transition as a function of treatment time at different temperatures: ●, 25; ○, 30; □, 35; ■, 40; ▽, 47.3°C

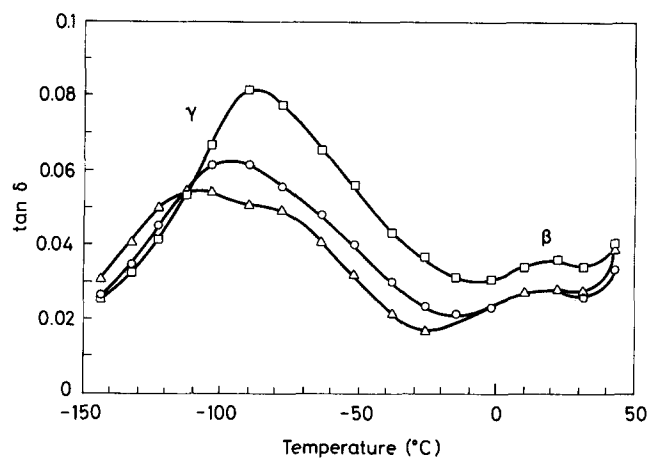


Figure 8 Dielectric loss tangent of PSLG measured after rapid cooling from 70°C:  $\Delta$ , 100 Hz;  $\circ$ , 1 kHz;  $\square$ , 10 kHz

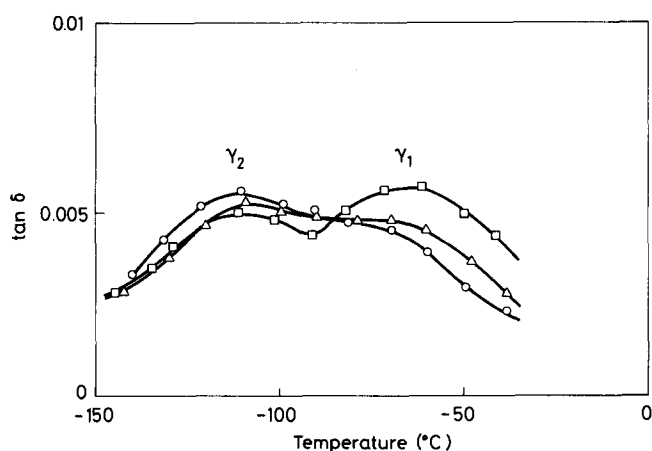


Figure 9 Tangent of dielectric damping of PSLG measured at 60 Hz after annealing for ( $\square$ ) 3.5 days at 47°C, ( $\Delta$ ) 3.5 days at 30°C and ( $\circ$ ) without isothermal treatment

temperature. The first, assigned to local movements of the side chains<sup>14,15</sup>, is similar in origin to those observed for polymethacrylates, polyacrylates or polyitaconates. The  $\beta$  relaxation is associated with the cooperative movement of the polymethylene segment as a whole group<sup>15,16</sup>, and corresponds to the pseudo glass transition of the side chains<sup>17</sup>. In PSLG, the  $\beta$  relaxation appears as a very low intensity peak (Figure 8). In polymers with 4–8 methylene units in the side chains, the  $\beta$  relaxation has a much higher intensity<sup>16,18</sup>, with values for the dielectric loss tangent around 10 times those observed for the  $\gamma$  relaxation. Such comparatively small values can be accounted for by assuming that the  $\beta$  relaxation occurs in side chains with no methylene unit in the crystalline phase, and indicates also that most side chains must participate in such a phase.

The  $\gamma$  relaxation of PSLG splits into two relaxations at frequencies  $< 1$  kHz, which we will call  $\gamma_1$  and  $\gamma_2$  in order of decreasing temperature. Their apparent activation energies are 26 and 11 kcal mol<sup>-1</sup>, respectively. Both the activation energy and the temperature at which it appears strongly suggest that the  $\gamma_2$  relaxation is associated with the single relaxation characteristic of poly(n-alkyl-L-glutamate)s with short side chains. The appearance of the  $\gamma_1$  relaxation is related to the crystallization process affecting the side chains. To evaluate the effect of crystallinity on these two relaxations

we have studied the dielectric spectrum of PSLG at 60 kHz after subjecting the sample to annealing at 47°C for 3.5 days ( $w_c = 0.34$ ) and at 30°C for 3.5 days ( $w_c = 0.36$ ), as well as a sample without annealing ( $w_c = 0.32$ ). The way in which the intensity of the  $\gamma_1$  relaxation increases with the crystalline fraction while that of the  $\gamma_2$  relaxation decreases is depicted in Figure 9.

We conclude that the  $\gamma_2$  relaxation can be attributed to a crankshaft type mechanism arising not only in completely amorphous side chains but also in those partially crystallized but containing at least six consecutive free methylene units. Indeed, the apparent activation energy which is measured fully agrees with that expected for this type of mechanism. Moreover, the crystalline fraction data lead us to expect that an average of 9–10 methylene units per side chain must remain in the amorphous phase. The striking intensification of the  $\gamma_1$  relaxation with a small increase in crystallinity may thus be interpreted as a consequence of the growth of the crystals hindering the molecular movement in an increasing number of chains. As the number of freely rotational C–C bonds is reduced to below the minimum necessary for the crankshaft mechanism to be able to operate, only the  $\gamma_1$  relaxation would occur. Its activation energy is presumed to be considerably greater and, therefore, appears at higher temperatures.

#### ACKNOWLEDGEMENTS

This work was supported in part by the CICYT (Projects no. PA-86-0218-C03-02 and no. MAT88-0555). We thank Mr J. Bou and Ms M. Garcia for assistance with g.p.c. and n.m.r. techniques, respectively, and Professor T. Yoshioka of the University of Tokyo, who kindly supplied the sample of PSLG.

#### REFERENCES

- 1 Watanabe, J., Ono, H., Uematsu, I. and Abe, A. *Macromolecules* 1985, **18**, 2141
- 2 Watanabe, J. and Ono, H. *Macromolecules* 1986, **19**, 1079
- 3 Yamanobe, T. et al. *Macromolecules* 1988, **21**, 48
- 4 Fatou, J. M. G. and Barrales Rienda, J. M. *J. Polym. Sci. A-2* 1969, **7**, 1755
- 5 Pakula, T. *Polymer* 1982, **27**, 1300
- 6 Avrami, M. *J. Chem. Phys.* 1939, **7**, 1103
- 7 Meseguer Dueñas, J. M., Gómez Ribelles, J. L. and Diaz Calleja, R. *J. Appl. Polym. Sci.* 1989, **37**, 1645
- 8 Colomer, P., Montserrat, S., Ribes, A., Meseguer, J. M., Gómez, J. L. and Diaz, R. *Polym. Plast. Technol. Eng.* 1989, **28**, 635
- 9 Flory, P. J. and Vrij, A. *J. Am. Chem. Soc.* 1943, **65**, 3548
- 10 Jordan, E. F., Feldeisen, D. W. and Wrigley, A. N. *J. Polym. Sci.* 1971, **9**, 1835
- 11 Barrales Rienda, J. M., Fernandez Martin, F., Romero Galicia, C. and Sanchez Chavez, M. *Makromol. Chem.* 1983, **184**, 2643
- 12 Sasaki, S., Miyamoto, M., Nakamura, T. and Uematsu, I. *Biopolymer* 1978, **17**, 2715
- 13 Sasaki, S., Nakamura, T. and Uematsu, I. *J. Polym. Sci.* 1979, **17**, 323
- 14 Matsushima, N., Masahira, K. and Kaneko, M. *J. Macromol. Sci. Phys.* 1973, **E8**(3–4), 413
- 15 Sasaki, N., Shimodate, H., Yamashita, Y. and Hikichi, K. *Polym. J.* 1979, **11**, 983
- 16 Kakizaki, M., Nakayama, H., Tanaka, H. and Hideshima, T. *Polym. J.* 1986, **18**, 141
- 17 Romero Colomer, F. and Gómez Ribelles, J. L. *Polymer* 1989, **30**, 949
- 18 Romero Colomer, F. Engn. Dr. Thesis, University Polytechnic of Valencia, Spain, 1989